IRSTI 29.17.35 https://doi.org/10.26577/JPEOS.2022.v24.i2.i3

M.S. Isataev, G. Toleuov, Zh.K. Seydulla*, A. Sagtagan, B. Rakhataeva
Al-Farabi Kazakh National University, Kazakhstan, Almaty
**e-mail: Zhanibek.seidulla@kaznu.kz*

INVESTIGATION OF THE VORTEX PICTURE OF A FREE JET FLOW BOUNDED BY FLAT WALLS

Abstract. It is shown that the aerodynamics of turbulent jets flowing from rectangular nozzles is significantly influenced not only by the presence or absence of limiting end walls, but also by the development of large-scale coherent vortices formed at the initial section of the jet. It is established that in the case of large-scale vortices formed at the initial section with axes parallel to the free edge of the nozzle, they can either rest against the end walls with their ends, or close on themselves at the end walls, covering the initial section of the jet. It is shown that the initially formed annular vortices covering the initial section of the jet deform as they move away from the nozzle and turn into vortex cords with axes parallel to the direction of the jet. As a rule, the vortex cords are arranged symmetrically relative to the axis and have opposite directions. These vortices are the main cause of the appearance of an uneven velocity and temperature profile along the axis. At the same time, large-scale primary vortices with their ends rest against the end walls and cannot cause the appearance of maxima and minima of the velocity profile along the axis. In this case, the development of the boundary layers at the end walls is similar to the development of the boundary layer of a homogeneous flow in a flat channel.

Key words: flat wall, vortex, Tepler's shadow installation, large-scale eddies, nozzle.

М.С. Исатаев, Г.К. Төлеуов, Ж.Қ. Сейдулла*, А. Сақтаған, Б. Рахатаева
Әл-Фараби атындығы Қазақ ұлттық университеті, Қазақстан, Алматы қ.
e-mail: Zhanibek.seidulla@kaznu.kz

Жазық қабырғалармен шектелген еркін ағынның ағыншадағы құйынды көрінісін зерттеу

Аннотация: Бұл жұмыста тікбұрышты саңылаулардан ағатын турбулентті ағындардың аэродинамикасына шектеуші қабырғалардың болуы немесе болмауы ғана емес, сонымен қатар ағынның бастапқы бөлігінде пайда болатын кең көлемді когерентті құйындардың дамуы да айтарлықтай әсер ететіндігі көрсетілген. Саңылаудың бос жиегіне параллель осьтері бар бастапқы аймақта пайда болған $\lambda \geq 10$ үлкен көлемді құйындар ұшымен соңғы қабырғаларға тірелуі мүмкін немесе ағынның бастапқы бөлігін қамтитын соңғы қабырғаларға жақын орналасуы мүмкін екендігі анықталды. Ағынның бастапқы бөлігін қамтитын алғашқыда пайда болған сақиналы құйындар саптамадан деформацияланып, ағынның бағытына параллель осьтері бар құйынды сымдарға айналатыны көрсетілген. Әдетте, құйынды сымдар z оське қатысты симметриялы орналасқан және қарама-қарсы бағытта болады. Бұл құйындар – жылдамдық пен температура профилінің z осьте біркелкі болмауының негізгі себебі. $\lambda \leq 7$ болған кездегі ірі масштабтағы алғашқы құйындар үшін олардың ұштары шеткі қабырғаларға тіреліп, z осі бойымен жылдамдық профилінің максимумдары мен минимумдарының пайда болуына жол бермейді. Бұл жағдайда соңғы қабырғалардағы шекаралық қабаттардың дамуы жазық каналдағы біртекті ағынның шекара қабатының дамуына ұқсас жүреді. Сонымен бірге амплитудалық-жиілік анализаторы әлдеқайда жоғары жиіліктерге дейінгі шағын масштабты жылдамдық пульсацияларының болуын көрсетеді.

Түйін сөздер: жазық қабырға, құйын, Теплер көлеңкелі қондырғысы, ірі масштабты құйындар, саптама.

М.С. Исатаев, Г.К. Толеуов, Ж.К. Сейдулла*, А. Сақтаган, Б. Рахатаева
Казахский национальный университет им. аль-Фараби, Казахстан, г. Алматы
e-mail: Zhanibek.seidulla@kaznu.kz

Исследование вихревой картины течения свободной струи, ограниченной плоскими стенками

Аннотация. В работе показано, что на аэродинамику турбулентных струй, истекающих из прямоугольных сопел, существенное влияние оказывает не только наличие или отсутствие ограничивающих торцовых стенок, но и развитие крупномасштабных когерентных вихрей, образующихся на начальном участке струи. Установлено, что при $\lambda \geq 10$ крупномасштабные вихри, образованные на начальном участке с осями, параллельными свободной кромке сопла, могут либо своими концами упираться в торцовые стенки, либо у торцовых стенок замыкаться сами на себя, охватывая начальный участок струи. Показано, что первоначально возникшие кольцевые вихри, охватывающие начальный участок струи, с удалением от сопла, деформируясь, превращаются в вихревые шнуры с осями параллельно направлению струи. Как правило, вихревые шнуры располагаются симметрично относительно оси z и имеют противоположные направления. Эти вихри являются основной причиной появления неравномерности профиля скорости и температуры по оси z. При $\lambda \leq 7$ крупномасштабные первичные вихри своими торцами упираются в торцовые стенки и не могут вызвать появление максимумов и минимумов профиля скорости по оси z. В этом случае развитие пограничных слоев у торцовых стенок происходит аналогично развитию пограничного слоя однородного потока в плоском канале.

Ключевые слова: плоская стенка, вихрь, теневая установка Теплера, крупномасштабные вихри, сопло.

Introduction

The visual picture of the flow in a plane jet was investigated with end walls made of glass. Visual pictures of the vortex structure were obtained using the Topler IAB-451 shadow setup. The optical inhomogeneity of the jet was achieved by slightly heating the jet. Along with this, a smoke jet with stroboscopic lighting was also used.

Instant photos of the shadow flow pattern in the jet with $\lambda = 16$ and $\lambda = 2.72$ at initial speed $U_0 = 5{,}4 м/\text{s}$ and various frequencies of acoustic exposure are shown in Figs. 1 and 2.

In the left half of all images, the light beam is directed parallel to the axis z (perpendicular to the end plates), on the right half - parallel to the axis y (parallel to the end plates). The left photographs clearly show large-scale vortices forming in the initial section parallel to the free edge of the nozzle.

In all images taken parallel to the axis z, in the initial section of the jet, large-scale vortices are visible, which become most intense at the resonance frequency corresponding to the value of the Strouhal number in the interval $\text{Sh} = 0{,}30 \div 0{,}50$. With distance from the nozzle further than the initial section, the shadow pattern of large-scale vortices is blurred and they become indistinguishable.

Analysis of the jet shadow pattern in the direction of the axis y (parallel to the end walls) shows that immediately after leaving the nozzle, the flow field is uniform in temperature along the axis oz. When $\lambda = 16$ already at a distance $\frac{x}{b} \geq 4$ longitudinal stripes appear, the contrast of which increases with distance from the nozzle and becomes uneven. The photographs show that helical vortices with an axis parallel to the direction of flow in the jet are formed at the end walls. Through their development over distances $\frac{x}{b} > 20$ three dark and two light flow stripes are formed in the right image in Fig. 1.

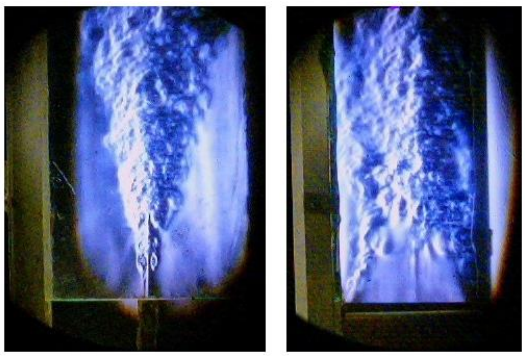

a – f = 100 *Hz;* Sh = 0,093 .

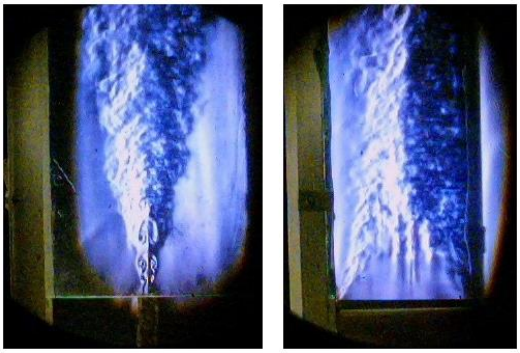

b – f = 320 Hz; Sh = 0,30 .

Figure 1 – Snapshots of the shadow pattern of a vortex flow in a plane jet with end walls at $\lambda = 16, U_0 = 5{,}4$ m / s.

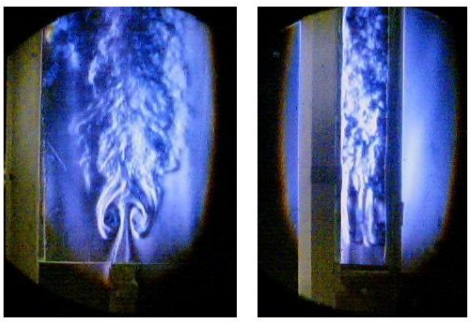

a – f = 62 Hz; Sh = 0,14.

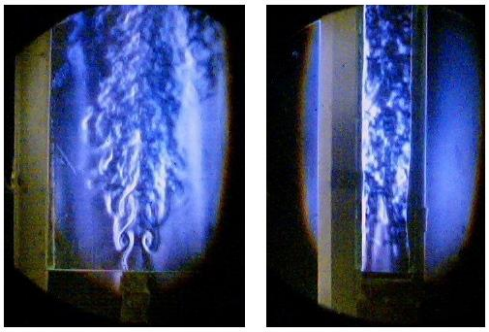

b - f = 125 Hz; Sh = 0,28.

Figure 2 – Snapshots of the shadow pattern of the vortex flow in a plane jet with end walls at $\lambda = 2{,}72$; $U_0 = 5{,}4$ m / s.

In this case, dark stripes correspond to areas with a low temperature, and light stripes correspond to areas with a higher temperature.

Obviously, these features of the motion of large-scale eddies can be explained as follows.

When $\lambda > 10$ large-scale vortices that have arisen in the initial section can either close on the end walls or close on themselves, covering the initial section of the jet in the form of a closed ring.

With the distance from the nozzle downstream, the near-wall part of the annular vortex at the end walls decelerates and lags behind the part of this vortex in the free mixing zone. As a result, the vortices are gradually deformed approximately as shown schematically in Figs. 3 and 4.

Projected onto a plane xz half of the vortex, facing the viewer, looks like an elongated arc with the legs below, in a plane xy - like an arc, turned upside down, and in a plane yz - like a vortex ring, deformed in the form of a figure eight. Such development of large-scale eddies leads to the formation of two maxima in the velocity and temperature profiles along the axis z .

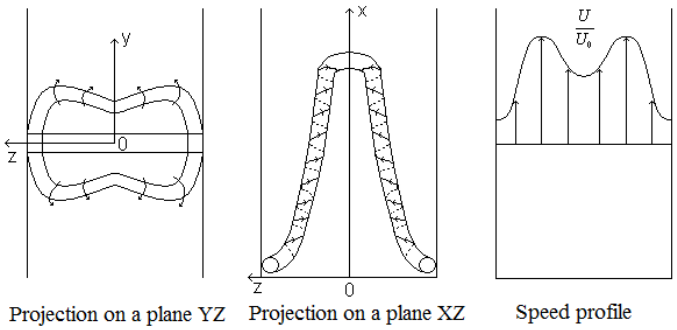

Figure 3 – Scheme of vortex development for $\lambda \approx 15$.

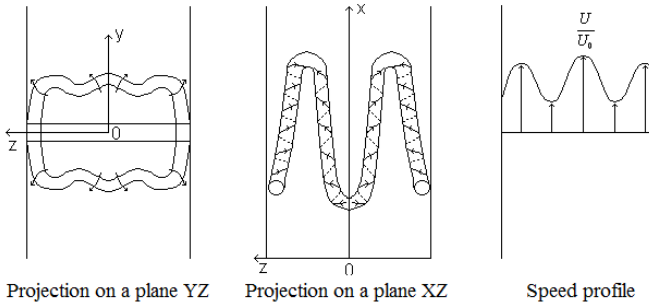

Figure 4 – Scheme of vortex development for $\lambda = 25$.

If the vortex deformation is realized as shown in Fig. 4, then this leads to the formation of three maxima in the profile of the velocity and excess temperature of the jet along the axis z.

The above results are qualitatively and quantitatively consistent with theoretical calculations of vortex clusters formed in the jet flow and in the wake of the body, performed by Z. Zh. Zhanabaev and coworkers [1, 2].

According to the calculations of the above authors, in the quadrupole structure of vortices, the distance between the centers of oppositely rotating vortices in one row corresponds to 10 calibers. If we take points corresponding to the mean value between the maximum and minimum values of the velocity as the centers of the vortices, then the distance between the centers of the vortices in one row at $\lambda = 16$ corresponds to 8.8 calibers, and the distance from the center of the extreme vortex to the wall is 3.7 calibers.

The same distances are maintained at $\lambda = 25$ when in one row along the axis z 4 oppositely rotating vortices are located.

With a small value $\lambda < 3 \div 5$ large-scale vortices that arise parallel to the nozzle edge in the free-mixing layer of the jet are closed at the end walls and they cannot cause non-uniformity of the velocity and temperature profile along the axis z.

In this case, the velocity profiles along the axis z between the end walls will develop in the same way as in a homogeneous flow in the initial section of a flat channel.

Figure 2 corresponding value $\lambda = 2{,}72$ shadow flow patterns in the direction of the axis z are qualitatively similar to the previous case for $\lambda = 16$. However, in the pictures in the plane xz (the ray is parallel to the axis y) spiral-screw motion of a vortex with an axis parallel to the jet flow is not observed.

Almost all visualization methods do not allow studying the development of discrete vortices that arise in the initial section, with distance from the nozzle in the main section of the jet. The ASCHKH-1 analyzer has a wide bandwidth and can register discrete frequencies of flow velocity fluctuations only within the initial section of the jet. Figure 5 shows a spectral analysis of turbulent velocity fluctuations in the initial section of a plane jet at a distance $\frac{X}{B} = 5$ and 40 for acoustic resonance exposure with a frequency $f = 320$ Hz in jet with parameters $\lambda = 16$ and $U_0 = 4{,}3\text{m/s}$.

As you can see, the analyzer at $\frac{X}{B} = 5$ shows not only the fundamental frequency of velocity oscillations caused by discrete vortices, but also harmonics corresponding to the frequencies $0{,}5f; 2f; 3f$ etc. On the spectrogram corresponding to the main section of the jet at a distance, $\frac{X}{B} = 40$ a continuous turbulent spectrum is visible.

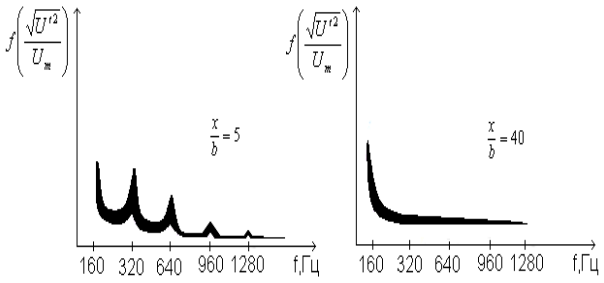

Figure 5 – Spectral analysis of turbulent pulsations speed at $f = 320$ Hz, $\lambda = 16$ and $U_0 = 4{,}3\text{m/s}$.

However, direct observation of the oscillograms of the instantaneous velocity pulsation signal sweep shows the presence of periodic velocity pulsations caused by primary large-scale vortices of the initial section of the jet. With moving away downstream, as a result of interaction and coalescence of the initial vortices into larger ones, low-frequency

structures with a larger amplitude of velocity fluctuations are formed. At the same time, high-frequency fluctuations of the velocity caused by the initial vortices are preserved against their background. For example, in Fig. 6 oscillograms of velocity pulsations in a jet bounded by end walls are presented for values of the parameter λ=16 and U_0=9,8m/s at different distances from the nozzle and from the jet axis.

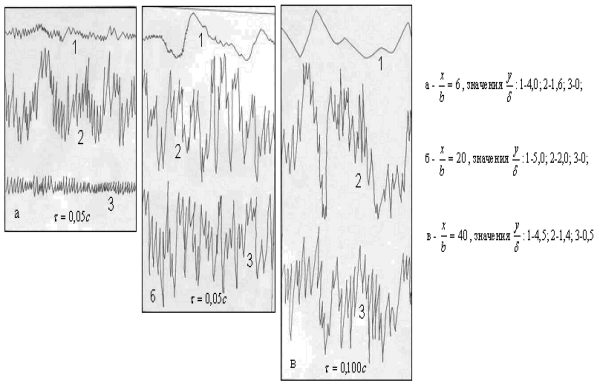

Figure 6 – Oscillograms of velocity pulsations in the jet at $\lambda = 16, U_0 = 9{,}8\text{m/s}$.

Waveform Sweep Time τ indicated in the figures. The frequencies of the primary vortices were calculated from the high-frequency pulsations, and the Strouhal numbers were calculated from them $\text{Sh}_0 = \frac{f\,2b}{U_0}, \text{Sh}_m = \frac{f\,2b}{U_m}$ (fig. 7).

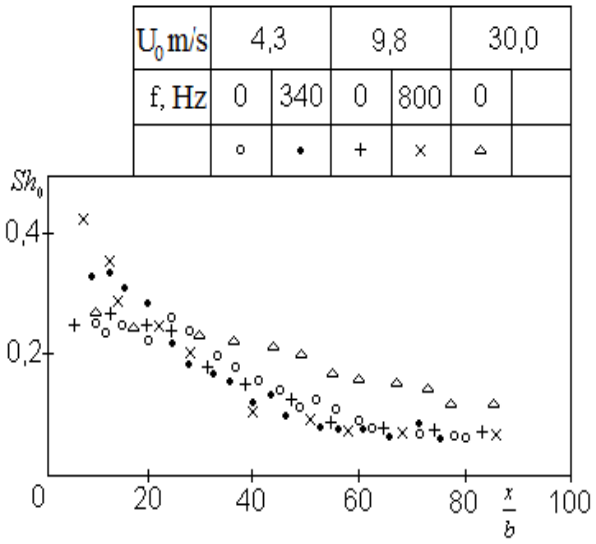

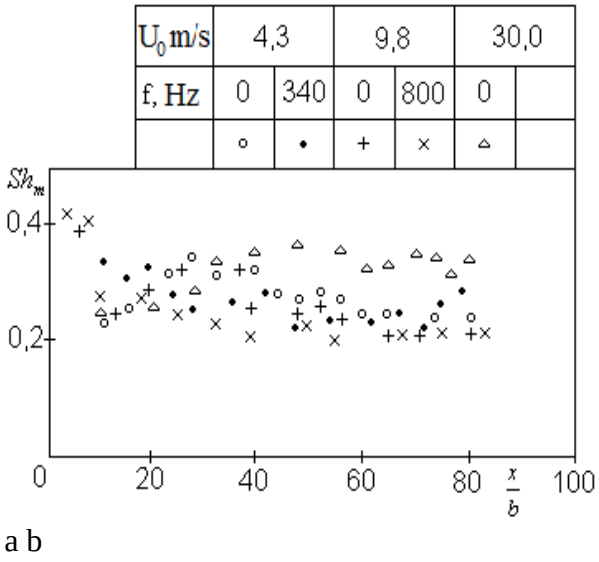

a b

Figure 7 – Changing the Strouhal number

Conclusion

As seen, Sh_0 decreases with distance from the nozzle. T his is due to the fact that as the flow velocity decreases with distance from the nozzle, the number of vortices passing by the hot-wire anemometer nozzle per unit time also decreases. Consequently Sh_m maintains an almost constant value along the length of the jet up to a large distance $\frac{X}{B} > 100$.

At the same time, it is very interesting that we established the fact that in an instantaneous oscillogram of velocity pulsations up to a large distance with a distance from the nozzle ($\frac{X}{B} > 100$) the frequency of small-scale pulsations does not exceed the frequency of the initial large-scale eddies of the initial section.

In this case, the amplitude of the pulsations of the velocity of primary vortices decreases by more than an order of magnitude in comparison with the amplitude of pulsations of large low-frequency vortex formations, which include up to tens of primary vortices.

At the same time, as you know, the amplitude-frequency analyzer shows the presence of small-scale velocity pulsations up to much higher frequencies.

This, obviously, is explained by the fact that any complex motion with continuously varying speed, according to the theory, can be represented by the Fourier series in the general

case as the sum of an infinite number of periodic trigonometric functions with increasing frequency and decreasing amplitude.

A similar phenomenon of preservation of a coherent vortex structure created by acoustic impact in a turbulent wake behind a thin plate and a profile far downstream was established in the work of N.N. Yanenko with colleagues [3,4] with a narrow-band amplitude-frequency analyzer total 4 *Hz.*

References

1. Zhanabaev Z.Zh., Mukhamedin S.M., Imanbaeva A.K. Informational criteria for the degree of self-organization in turbulence. // Izvestiya vuzov. Physics - 2001, No. 7, P.72-77.

2. Zhanabaev Z. Zh., Tarasov S.B. Imanbaeva A.K., Almasbekov N.E. On the dynamics of interacting vortices. // Thermophysics and Aeromechanics. - 2002. Vol.9, No. 2 - S. 201-211.

3. Yanenko N.N., Bardakhanov S.P., Kozlov V.V. Formation of coherent structures in a turbulent wake under acoustic impact. - Dokl. USSR Academy of Sciences, 1984, v.274, No. 1. S.50-53.

4. Bardakhanov S.P., Kozlov V.V., Yanenko N.N. Transformation of acoustic disturbances into coherent structures in a turbulent wake behind the airfoil. - IFZh, 1984, vol. 47, No. 4, pp. 533-536.

Принято в печать 05.10.2022